National University of Science and Technology POLITEHNICA Bucharest
Doctoral School of Chemical Engineering and Biotechnologies

PhD Thesis Abstract

Functionalized platforms for the control, modulation, and detection of biologically active agents

PhD Supervisor:
Prof. dr. Ing. Cristian Pîrvu

Author :
Drd. Ing. Alexandra Constantinescu

Bucharest, 2025

Functionalized platforms for the control, modulation, and detection of biologically active agents

TABLE OF CONTENTS

I. CURRENT STATE OF KNOWLEDGE IN THE FIELD
Chapter 1. Introduction 14
1.1. Scientific and applied context 14
1.2. Motivation of the PhD thesis 15
1.3. Objectives and structure of the thesis 17
General objective 17

Chapter 2. Biomaterials and functionalized matrices for tissue regeneration and control of biologically active agents 20
2.1. Introductory notions on biomaterials 20
2.2. Properties of biomaterials 22
2.3. Nanostructured biomaterials 23
2.4. Biomolecular interactions 24
2.5. Biomaterial design 25
2.6. Use of titanium alloys for biomedical applications 27
2.7. Bioactive compounds of interest and their interaction with functionalized surfaces and matrices 28
2.7.1. Zinc oxide 28
2.7.2. Amoxicillin 30
2.7.3. D-Fructose 30

Chapter 3. Functionalized surfaces: modification and characterization techniques 34
3.1. Surface modification techniques 34
3.1.1. Functionalization by nanostructuring 34
3.1.2. Functionalization by electrospinning 37
3.1.3. Functionalization by anodic oxidation 38
3.1.4. Functionalization by constant-current deposition 40
3.1.5. Functionalization by constant-potential deposition 40
3.1.6. Functionalization by potentiodynamic polarization 41

3.2. Surface characterization techniques 42
3.2.1. Characterization by non-electrochemical techniques 42
3.2.1.1. Characterization by contact angle analysis 42
3.2.1.2. Characterization by Atomic Force Microscopy (AFM) 44
3.2.1.3. Characterization by SEM analysis – morphology, feature size, layer thickness 46
3.2.1.4. Characterization by EDS/EDX analysis – surface elemental composition 46
3.2.1.5. Characterization by FT-IR analysis 46
3.2.1.6. Characterization by DLS analysis 47
3.2.1.7. Characterization by Vickers microhardness 48
3.2.1.8. Characterization by XRD analysis 48
3.2.1.9. Characterization by UV–Vis spectroscopy 50

3.2.2. Characterization by electrochemical techniques 52
3.2.2.1. Characterization by cyclic voltammetry (CV) 52
3.2.2.2. Characterization by differential pulse voltammetry (DPV) 53
3.2.2.3. Characterization by electrochemical impedance spectroscopy (EIS)

..... 54
3.2.2.4. Characterization by Mott–Schottky (M–S) analysis 59
3.2.2.5. Characterization by chronoamperometry (CA) 60
3.2.2.6. Characterization by chronopotentiometry (CP) 61
3.2.2.7. Characterization by Tafel analysis 61

Chapter 4. Testing of functionalized surfaces and matrices in biomedical applications 63
4.1. Introduction 63
4.2. Testing of antibacterial effects 64
4.2.1. Biomedical-relevant bacterial types and biofilm complexity 64
4.3. Analytical testing by Surface Plasmon Resonance (SPR) 66
4.3.1. Electrochemically coupled surface plasmon resonance (EC-SPR): principles and applications 67
4.4. Performance parameters (LoD, LoQ, and calibration curve) 68

II. ORIGINAL RESEARCH

Chapter 5. Control and modulation of antibacterial activity through surface properties 70
5.1. Introduction 70
5.2. Materials and reagents 71
5.3. Surface coating/modification and characterization protocol 72
5.3.1. Surface modification protocol 72
5.3.1.1. Cleaning 72
5.3.1.2. Anodic oxidation 72
5.3.1.3. Electrodeposition 73
5.3.1.4. Calcination 73

5.3.2. Surface characterization techniques 73
5.3.2.1. Scanning electron microscopy (SEM) 73
5.3.2.2. Atomic force microscopy (AFM) 73
5.3.2.3. Contact angle and surface energy analysis 74
5.3.2.4. UV–Vis–NIR spectroscopy 74
5.3.2.5. Zinc ion release 74
5.3.2.6. Vickers microhardness 74

5.3.3. Evaluation of antimicrobial effects 75
5.3.3.1. Growth rate inhibition (I, %) 75
5.3.3.2. Determination of bactericidal ratio (R, %) 75

5.4. Results and discussion 76
5.4.1. Surface modification by nanostructuring 76
5.4.1.1. Nanostructuring by anodic oxidation 76
5.4.2. Nanostructuring by electrochemical deposition of zinc oxide (ZnO) 77

5.5. Surface characterization 82
5.5.1. Contact angle and surface energy analysis 82
5.5.2. AFM analysis 84
5.5.3. Electrical double-layer capacitance (Cdl) 86

5.5.4. Electrochemical impedance spectroscopy (EIS) 88
5.5.5. Tafel analysis 89
5.5.6. Zinc ion release 90
5.5.7. Vickers microhardness 91
5.5.8. UV–Vis spectroscopy, optical band gap, and Tauc plot 93
5.5.9. Antibacterial activity 95

5.6. Partial conclusions 98

Chapter 6. Detection of *Escherichia coli* by electrochemically coupled surface plasmon resonance (EC-SPR) 99
6.1. Introduction 99
6.2. Experimental section 100
6.2.1. Materials and reagents 100
6.2.1.1. Instrumentation 100
6.2.1.2. Phytosynthesis of gold nanoparticles (AuNPs) 100
6.2.1.3. Modification of SPR electrodes 101

6.3. Results and discussion 101
6.3.1. Electrochemical and SPR evaluation of *E. coli* on the gold electrode 101
6.3.2. Electrochemical and SPR evaluation of *E. coli* on AuNP-modified gold electrodes 102
6.3.2.1. FT-IR spectroscopic characterization of phytosynthesized AuNPs 102
6.3.2.2. Modification of the gold electrode with phytosynthesized AuNPs and EC-SPR signal 103

6.3.3. Sensitivity and linearity of the EC-SPR response in *E. coli* detection on the modified gold electrode 105

6.4. Partial conclusions 108

Chapter 7. Amoxicillin detection on electrodes functionalized with ZnO nanostructures obtained from silk fibroin 109
7.1. Introduction 109
7.2. Materials and methods 109
7.2.1. ZnO preparation 109
7.2.2. Modification of glassy carbon electrodes 110
7.2.3. ZnO structures and characterization of modified electrodes 110
7.2.4. Amoxicillin detection 111

7.3. Results and discussion 111
7.3.1. Characterization of the modified electrode 111
7.3.2. Selection of the appropriate voltammetric method for AMX detection 114
7.3.3. Signal enhancement for AMX detection 117
7.3.4. Calibration curve 118

7.4. Partial conclusions 119

Chapter 8. Carbon Quantum Dot–Modified Electrodes for D-Fructose Detection 121
8.1. Introduction 121
8.1.1. Chemicals and reagents 121
8.1.2. Materials and methods 121
8.1.3. Carbon quantum dot synthesis 122
8.1.4. Preparation of modified electrodes 122
8.1.5. Characterization of carbon quantum dots 124

8.2. Results and discussion 125
8.3. Partial conclusions 129

Chapter 9. Conclusions 130

References 133

I. CURRENT STATE OF KNOWLEDGE IN THE FIELD

Chapter 1. Introduction

1.1. Scientific and Applied Context

Infections associated with medical devices represent one of the most significant challenges of modern biomaterials and clinical medicine, with an incidence that continues to increase proportionally to the number of implants used in orthopedics, dentistry, cardiology, or urology [1, 2]. Implantable materials, although designed to be biocompatible, are inherently vulnerable to microbial colonization because, unlike living tissues, they lack local immune mechanisms, vascularization, and the ability to eliminate biological intruders. [1, 2].

Immediately after implantation, the biomaterial comes into contact with blood and tissue fluids, triggering a series of extremely rapid interfacial processes. Within the first seconds, serum proteins such as albumin, fibrinogen, fibronectin, and immunoglobulins adsorb onto the surface according to the Vroman model, in a sequence governed by their mobility, concentration, and affinity [3]. This layer of adsorbed proteins completely redefines the surface identity, meaning that bacteria do not interact with the material itself, but with a newly formed biological layer [3]. The orientation, structure, and composition of these proteins determine whether the surface becomes favorable for bacterial colonization or allows human cells to initiate the normal process of osseointegration [4].

The competition between bacteria and host cells for surface colonization is a decisive phenomenon, and its outcome depends on the physicochemical properties of the biomaterial, local conditions, and the initial bacterial concentration [5]. If bacteria succeed in anchoring first, the process of biofilm formation is initiated and becomes almost impossible to interrupt. A biofilm represents an organized three-dimensional system composed of microorganisms embedded in an extracellular matrix of polysaccharides, proteins, and lipids, exhibiting mechanical and chemical properties that confer resistance to both antimicrobial drugs and the immune system [4, 5] .

The antibiotic resistance conferred by biofilms is dramatically increased—by 10 to 1000 times compared to planktonic bacteria—due to a complex set of mechanisms, including limited antibiotic diffusion, reduced metabolic activity of bacteria in deeper layers, and modulation of resistance gene expression [6]. These factors explain why chronic implant-associated infections are difficult to treat and why the final solution is often surgical removal of the implant, which entails increased morbidity, high costs, and significant therapeutic risk [7].

Functionalized platforms for the control, modulation, and detection of biologically active agents

In this context, the need to develop functionalized surfaces becomes evident—surfaces capable not only of resisting bacterial colonization but also of playing an active role in infection prevention[8] [8]. The implant surface, from composition to topography, must be designed to intervene at critical stages of microbial adhesion [4, 9]. With the evolution of nanomaterials, it has become possible to integrate multiple functions into surface architectures: anti-adhesive properties, mechanical or chemical bactericidal activity, generation of reactive oxygen species, and even electrochemical platforms for bacterial detection [4, 9].

One emerging direction is the concept of smart implants, capable of monitoring the local environment and instantaneously signaling the presence of bacteria or infection-specific metabolites [10, 11]. The integration of electrochemical sensors directly onto the biomaterial surface enables early detection of amoxicillin, microbial metabolites, or compounds such as D-fructose, which is metabolically involved in certain inflammatory and infectious processes [12]. This digitalization of biomaterial surfaces, combined with antibacterial functionalization, represents a strategic evolution in the prevention of implant-associated infections [13].

Motivation of the PhD Thesis

Despite major advances in the field of biomaterials and biomedical engineering, clinical outcomes are still frequently limited by interactions at the interface between the material and living tissue. Two interconnected challenges dominate this interface:

1. the prevention of microbial colonization and biofilm formation on implants and medical devices;
2. the remodeling of tissue functional architecture and signaling, particularly for tissues with limited regenerative capacity, such as cartilage.

Prosthetic joint infection remains rare but devastating; once established, biofilm-associated infection is difficult to eradicate, as bacteria embedded in biofilms become protected from both antibiotics and the host immune defenses, often requiring complex revision surgeries and prolonged treatment [14, 15]. This clinical reality motivates the development of interfaces that are not merely inert, but actively resist bacterial attachment while maintaining surface chemistry and structures compatible with host integration.

One aspect that emerges clearly from the literature is that antibacterial performance is rarely dictated by a single surface characteristic. Instead, bacterial attachment and killing are modulated by a coupled set of parameters, including nanoscale topography, microscale roughness, surface energy and wettability, electrochemical behavior, and the presence of bioactive nanophases capable of inducing oxidative stress or membrane imbalance[15-18]. At the same time, host cells respond to many of the same cues. Consequently, the design of a clinically relevant surface requires optimization within a multidimensional parameter space, in which antibacterial and regenerative requirements must be balanced rather than independently maximized.

Functionalized platforms for the control, modulation, and detection of biologically active agents

In this context, the study of functionalized surfaces on titanium alloys addresses a central gap: how multiple surface properties interact to systematically modulate antibacterial efficacy. Titanium-based alloys are widely used due to their corrosion resistance and biocompatibility, yet they remain susceptible to bacterial adhesion, particularly under physiological conditions where early colonization can initiate biofilm formation. In the study of Ti50Zr, controlled electrochemical techniques were employed to engineer distinct anodic oxide morphologies (compact oxide, nanotubes, and nanochannels) and to further introduce ZnO as a bioactive phase, creating composite interfaces designed to disrupt bacterial viability. Importantly, the antibacterial outcomes did not simply follow a single-variable trend, such as wettability. Instead, the overall conclusions support a multiparametric view: morphology-dependent effects (e.g., nanochannels providing a distinct interaction mode compared to nanotubes) combine with ZnO-related mechanisms (e.g., nanoparticle size and distribution) to produce the strongest antibacterial response. In parallel, ZnO nanostructures are widely recognized for their antibacterial activity through the generation of reactive oxygen species, local membrane interactions, and Zn^{2+} release, with effectiveness strongly influenced by particle size and surface chemistry. These insights provide a solid scientific basis for the development of multifunctional interfaces as a pathway toward infection-resistant metallic biomaterials. However, anti-infective function alone is not sufficient for next-generation biomedical systems.

A second major motivation of the thesis is that prevention and treatment should be coupled with monitoring: infection biomarkers, pathogen load, and relevant therapies should ideally be tracked in real time. Conventional microbiological methods are often slow, while clinical symptoms may appear only after significant colonization has already occurred. This motivates detection strategies capable of monitoring pathogenic bacteria and pharmaceutical compounds with high sensitivity and operational simplicity.

The research presented in this PhD thesis contributes to this need through two complementary detection directions. First, a label-free EC-SPR approach was developed, based on green-synthesized gold nanoparticles (AuNPs) obtained using broccoli extract, integrated onto a gold disk electrode and applied to the detection of *E. coli*. Optical/electrochemical transduction is attractive because it can record interfacial binding events without the need for complex labeling and can be adapted for rapid pathogen screening. Second, an electrochemical platform for amoxicillin detection was developed, based on ZnO nanostructures obtained from silk fibroin and incorporated into a Nafion film on a glassy carbon electrode. Electrochemical detection of antibiotics is motivated by both clinical and environmental factors: antibiotics are essential for infection management, yet their overuse and persistence contribute to resistance selection, while their detection in relevant matrices remains analytically challenging. Nafion-based films are widely used in electroanalytical chemistry because their ionic selectivity and antifouling behavior can enhance signal stability and reduce interferences, which is particularly valuable in complex samples. Together, these two detection directions (pathogen detection and antibiotic monitoring) support the broader vision of the thesis, in which functional biomaterials are integrated with analytical platforms.

Functionalized platforms for the control, modulation, and detection of biologically active agents

Another direction that complements this detection platform framework concerns sugar detection and its biomedical relevance, using D-fructose as a model. Although glucose is the most extensively studied monosaccharide, fructose is increasingly discussed as a marker/indicator in metabolic and nutritional contexts (including urine or food samples), and its selective detection remains challenging due to interferences and structural similarity to other monosaccharides.

In the work dedicated to D-fructose, architectures based on polypyrrole, Nafion, and carbon quantum dots (CQDs) were employed, and both electrochemical impedance spectroscopy (EIS) and square-wave voltammetry (SWV) were evaluated for analytical response. The results highlighted that the simple addition of CQDs does not automatically guarantee increased sensitivity, reinforcing the central idea of the thesis: performance is governed by the interaction between composition, morphology, and transport, and must be rationally optimized. The literature supports this direction, as there are reported examples of monosaccharide detection by EIS using functionalized materials. Thus, this research is positioned within a field where selectivity and stability can be achieved either through recognition elements or through interfacial and ionic/electronic transport engineering.

Therefore, the motivation of my doctoral research is the unification of these directions into a coherent framework of interface engineering for biomedical applications:

- Nanostructuring and functionalization of metallic surfaces (Ti50Zr) to control bacterial colonization and to understand topography-/chemistry-dependent mechanisms;
- Development of detection platforms (electrochemical and optical) capable of quantifying bacteria or bioactive molecules with clinical and environmental relevance.

In all these systems, performance is not determined by a single material or a single technique, but by the correlation between morphology, composition, ionic/electronic transport, and experimental conditions. The thesis aims to transform this correlation into a methodology: controlled interface definition, quantitative measurement (EIS/CV/DPV/EC-SPR), statistical validation, and detailed interpretation, so that the results can be transferred toward biomaterial applications and detection platforms.

Objectives and Structure of the Thesis

General Objective

- Development, functionalization, and characterization of biomaterial surfaces and matrices for the control, modulation, and detection of biologically active agents (bacteria and bioactive compounds such as amoxicillin and D-fructose), using advanced

surface modification techniques, physicochemical characterization, and electrochemical methods.

Specific Objectives

- Development and optimization of surface functionalization procedures through nanostructuring (anodic oxidation), electrochemical deposition of ZnO, and thermal treatments on titanium alloys, in order to obtain surfaces with controllable morphological, chemical, and electrochemical properties and antibacterial effects.
- Comprehensive characterization of functionalized surfaces and matrices using morphological, structural, optical, and mechanical techniques (SEM, AFM, contact angle, UV–Vis, XRD, microhardness, Zn^{2+} release), as well as electrochemical methods (CV, DPV, EIS, Mott–Schottky, CA, Tafel), and correlation of these results with the functionalization process and interactions with biologically active agents.
- Evaluation and control of the antibacterial activity of nanostructured and ZnO-coated surfaces through specific tests (growth rate inhibition, bactericidal ratio), and correlation of antibacterial response with surface properties.
- Development of EC-SPR platforms for the detection of Escherichia coli on unmodified gold electrodes and gold electrodes modified with phytosynthesized gold nanoparticles.
- Design and testing of electrochemical platforms for the detection of bioactive compounds through the development of electrodes functionalized with ZnO nanostructures (for amoxicillin detection) and Carbon Quantum Dots (for D-fructose detection).

Thesis Structure

The thesis is structured into two main parts: **Part I**, which represents the literature review (Chapters 1, 2, 3, and 4), and **Part II**, which presents the original contributions (Chapters 5, 6, 7, and 8). The conclusions of the doctoral thesis are presented in **Chapter 9**.

Chapter 1 addresses the problem of implant-associated infections and the critical role of the material–tissue interface: bacteria/host cell competition, biofilm formation, and the limitations of antibiotic therapy. The need for functionalized surfaces and "smart implants" that combine antibacterial properties with detection functions is justified. The general and specific objectives are defined: nanostructuring of Ti50Zr alloys, development of EC-SPR platforms for *E. coli*, electrochemical sensors for amoxicillin and D-fructose, and correlation of performance with surface properties.

Chapter 2 represents the theoretical synthesis section: biomaterials, biocompatibility, implants, mineralization, osteoconduction, and osteoinduction are defined, with emphasis on the role of surface chemistry and topography. Essential chemical and physicochemical properties (hydrophilicity, surface energy, degradation, immune response) are described,

followed by a discussion of nanostructured biomaterials, nanomaterial classification (0D–3D), and biomolecular interactions (protein adsorption, cell adhesion, enzymatic degradation, immune response). Principles of biomaterial design (smart polymers, surface functionalization, bioconjugation) and the role of Ti–Zr alloys in biomedical applications are presented, along with three classes of bioactive compounds of interest in this thesis: ZnO, amoxicillin, and D-fructose.

Chapter 3 presents the techniques used to modify and analyze surfaces: nanostructuring (including anodic oxidation), electrochemical deposition at constant current/potential, and potentiodynamic polarization. Characterization methods include non-electrochemical techniques (contact angle, AFM, SEM/EDS, FT-IR, DLS, Vickers microhardness, XRD, UV–Vis) and electrochemical techniques (CV, DPV, EIS, Mott–Schottky, CA, and Tafel analysis), which are later used to correlate surface structure and chemistry with antibacterial and analytical responses.

Chapter 4 describes relevant bacterial types and biofilm formation, followed by methodologies for antibacterial testing (growth rate inhibition, bactericidal ratio). The second part introduces the principles of Surface Plasmon Resonance (SPR) and EC-SPR, as well as analytical performance parameters LoD and LoQ, including their determination from calibration curves and the role of surface chemistry in detection platforms.

Chapter 5 presents the fabrication of Ti50Zr alloys with three types of anodic oxide (compact oxide, nanotubes, nanochannels) and the subsequent deposition of ZnO by pulsed electrodeposition and calcination. The surfaces are analyzed morphologically (SEM, AFM), by contact angle/surface energy, electrical double-layer capacitance (C_{dl}), EIS, Tafel analysis, microhardness, optical band gap, and Zn^{2+} release. The results demonstrate that antibacterial response does not depend on a single parameter (e.g., wettability alone or Zn^{2+} alone), but on a combination of nanoscale topography, electrochemical properties, and ZnO distribution. ZnO-coated nanochannels provide the best compromise between nanostructuring and antibacterial activity.

5.5.3. Electrical Double-Layer Capacitance (C_{dl})

At the biomaterial–electrolyte interface, the relationship between surface charge and the oxide–solution interface influences the electrical double-layer capacitance (C_{dl}), which is an essential characteristic governing surface interactions. Previous studies have highlighted the role of the electrical double layer in bacterial adhesion, as bacterial cell surfaces are generally negatively charged under physiological conditions, which can induce electrostatic repulsion when approaching negatively charged titanium alloy surfaces.

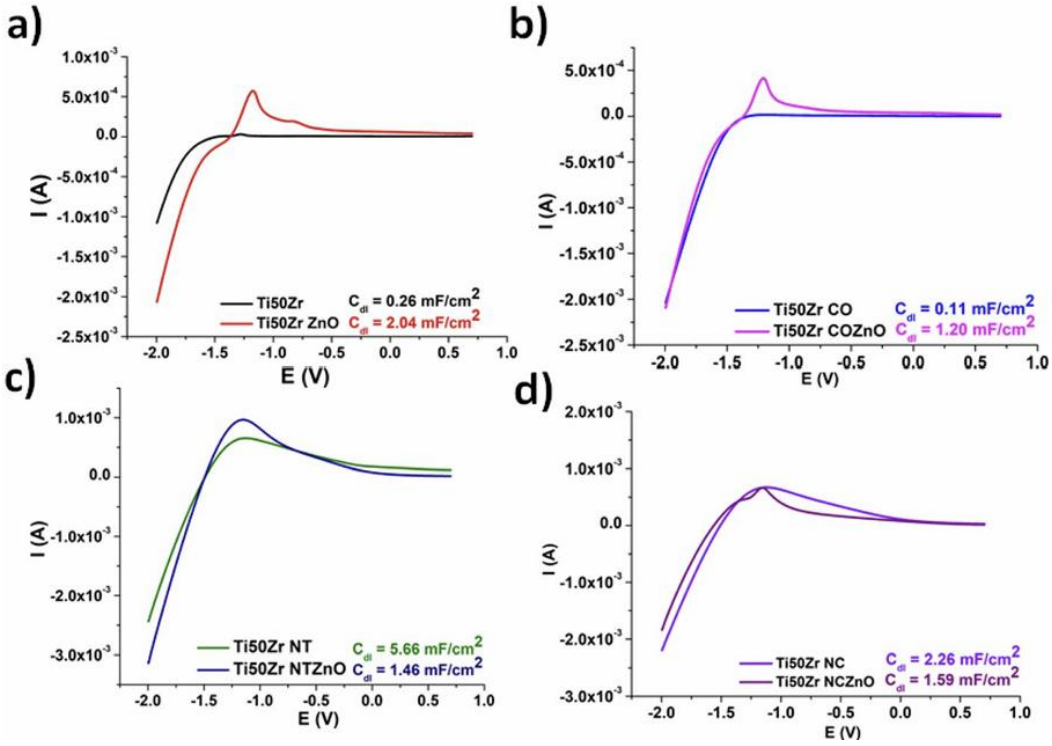


Figure 33. *Anodic branch of the cyclic voltammograms used for Cdl calculation, corresponding to the samples: (a) Ti50Zr and ZnO-coated, (b) Ti50Zr CO and ZnO-coated, (c) Ti50Zr NT and ZnO-coated, and (d) Ti50Zr NC and ZnO-coated.*

After the first surface modification step, the formation of a compact oxide layer on the Ti50Zr alloy smoothed the surface, reducing the active area and decreasing Cdl (***Figure 33a*** and ***b***). In contrast, nanostructuring Ti50Zr with a porous nanotubular (NT) layer improves surface wettability and roughness, favoring charge transfer and electrical double-layer formation. The increased roughness and porosity of Ti50Zr NT and Ti50Zr NC contribute to higher C_{dl} values, particularly for Ti50Zr NT (5.66 mF·cm^{-2}), suggesting more efficient ionic adsorption and desorption. Ti50Zr NC, despite exhibiting higher roughness and S_{dr}, shows a lower C_{dl} (2.26 mF·cm^{-2}), likely due to the smaller dimensions of the nanochannels and an intermediate surface state between the Cassie and Wenzel wetting regimes.

In the second modification step, ZnO deposition on the Ti50Zr surface increases the Cdl value (***Figure 33a***). This behavior is commonly observed for metal oxide coatings, as illustrated by Ti50Zr CO, where pulsed electrochemical deposition of Zn and subsequent formation of ZnO rod-like structures increase the active surface area and Cdl (from 0.11 to 1.2 mF·cm^{-2}). However, for Ti50Zr NTZnO and Ti50Zr NCZnO, Cdl decreases after ZnO deposition. This reduction is most likely due to decreased surface roughness, as indicated by AFM analysis, where ZnO deposition on the walls and interspaces of nanotubes and nanochannels reduces the effective active surface area.

5.5.9. Antibacterial Activity

The antibacterial activity of Ti50Zr samples modified with different surface structures and coatings was evaluated using growth rate inhibition tests and the bactericidal ratio assay. The unmodified Ti50Zr substrate (C*) exhibited the lowest inhibition rate against *E. coli* (20%), as shown in ***Table 9***. Surface modifications significantly enhanced the antibacterial properties, with Ti50Zr NC nanostructures (needle-like morphologies) showing the highest inhibition rate of 60%, representing a +41% improvement compared to the unmodified substrate. ZnO coatings further amplified the antibacterial effect. Specifically, Ti50Zr NCZnO exhibited the best antibacterial performance, with an inhibition rate of 75%, while Ti50Zr NTZnO showed an inhibition rate of 71%, corresponding to a +47% increase compared to Ti50Zr NT. The results obtained using the two evaluation methods are very close in value, indicating good consistency between the assays.

Table 9. *Antibacterial activity. Growth rate inhibition (%) and bactericidal ratio (%).*

Sample	Inhibition rate (%)	Bactericidal ratio (%)
Ti50Zr	C*	C*
Ti50Zr ZnO	57	56
Ti50Zr CO	20	21
Ti50Zr COZnO	54	55
Ti50Zr NT	24	25
Ti50Zr NTZnO	71	70
Ti50Zr NC	60	63
Ti50Zr NCZnO	75	77

Surface modification of Ti50Zr significantly influenced surface characteristics such as hydrophobicity, surface energy, roughness, and capacitance (C_{dl}), which in turn affect bacterial adhesion. As summarized in ***Table 10***, Ti50Zr NT, which exhibited the highest surface energy and the greatest hydrophobicity, did not show a major improvement in antibacterial efficiency (24% inhibition rate, 25% bactericidal ratio).

Table 3. *Comparative features of anodized samples (Ti50Zr CO, Ti50Zr NT, and Ti50Zr NC) relative to the Ti50Zr substrate.*

Features	Ti50Zr CO *vs.* Ti50Zr	Ti50Zr NT *vs.* Ti50Zr	Ti50Zr NC *vs.* Ti50Zr
Hydrophilicity	Slightly more hydrophilic (+)	More hydrophilic (+++)	More hydrophilic (++)
Surface energy	The same (=)	Higher (++)	Higher (+)
Roughness (R_{ms})	Lower (−)	Higher (+)	Higher (++)
C_{dl}	Lower (−)	Higher (++)	Higher (+)
Morphology (oxide nanostructuration)	Compact oxide	Nanotubes	Nanochannels
Antibacterial efficiency	Slightly higher	Slightly higher	Higher
Inhibition rate, I (%)	(20%)	(24%)	(60%)
Bacetericidal ratio, R (%)	(21%)	(25%)	(63%)

[a] Number of (+)/(−) indicates the increase/decrease order of the parameters compared to the reference sample. (=) means similar values.

Despite the fact that Ti50Zr NTZnO exhibits the lowest ZnO surface content and the lowest release of Zn^{2+} ions (1.37×10^{-5} mol L^{-1}), it showed the greatest improvement in antibacterial efficiency, highlighting that surface morphology, particularly the presence of small ZnO nanoparticles, can be a more important factor than the total amount of ZnO present or the surface energy.

Table 4. *Comparative features of ZnO-coated samples versus uncoated samples.*

Features	Ti50Zr ZnO *vs.* Ti50Zr	Ti50Zr COZnO *vs.* Ti50Zr CO	Ti50Zr NTZnO *vs.* Ti50Zr NT	Ti50Zr NCZnO *vs.* Ti50Zr NC
Hydrophilicity	Slightly less hydrophilic (−−)	Hydrophobic (−−−)	Slightly less hydrophilic (−)	Hydrophobic (−−−−)
Surface energy	Higher (++)	Higher (++++)	Slightly higher (+)	Higher (+++)
Roughness	Higher (++++)	Higher (+++)	Lower (−−)	Lower (−)
C_{dl}	Higher (++)	Higher (+)	Lower (−)	Lower (−−)
Morphology (ZnO nanostructuration)	Nanorods (∼80 nm)	Rods (∼200 nm)	Nanoparticles (∼10 nm)	Nanorods (∼80 nm)
Zn surface content (EDS)	(+++)	(++++)	(++)	(+)
Zn^{2+} ion release	(++++)	(+++)	(+)	(++)
Antibacterial efficiency	Higher (+38%)	Higher (+34%)	Higher (+47%)	Higher (+15%)

[a] Number of (+)/(−) indicates the increase/decrease order of the parameters compared to the reference sample.

Table 11 also shows that Ti50Zr ZnO and Ti50Zr COZnO exhibited similar antibacterial efficiencies (+38% and +34%, respectively), whereas Ti50Zr NCZnO displayed a more modest improvement in antibacterial performance. This suggests that the combination of surface morphology obtained in the first modification step and ZnO deposition in the second step plays a significant role in amplifying antibacterial activity, with sharp nanostructures enabling more effective bacterial inhibition.

From a statistical perspective, CFU values varied considerably among the tested surfaces. The uncoated Ti50Zr control exhibited the highest bacterial adhesion (mean CFU = 522), confirming its limited antibacterial properties.

Among the modified samples, Ti50Zr NCZnO exhibited the most effective antibacterial behavior, with a significant reduction in CFU (mean = 120 ± 5.7), corresponding to an inhibition rate of approximately 75%. Similarly, Ti50Zr COZnO demonstrated strong antibacterial effects

(mean = 157 ± 1.5). In contrast, samples such as Ti50Zr NTZnO and Ti50Zr ZnO showed moderate reductions in CFU but did not differ statistically significantly from the control.

Chapter 6 develops an EC-SPR platform based on an SPR gold electrode modified with phytosynthesized gold nanoparticles obtained from broccoli extract. The synthesis and characterization of the AuNPs (FT-IR, SEM), electrode modification, and combined electrochemical/SPR measurements for *E. coli* on both unmodified and modified electrodes are presented. The AuNP-coated electrode exhibits superior sensitivity and linearity, with low LoD and LoQ values achieved without the use of antibodies or aptamers, demonstrating the feasibility of rapid, label-free detection of low bacterial loads in food, environmental, or clinical contexts.

6.3. Results and Discussion

6.3.1. Electrochemical and SPR Evaluation of *E. coli* on the Gold Electrode

Previous studies have shown that bacterial membranes, including those of *E. coli*, carry a net negative charge under physiological conditions [19]. Therefore, the application of a positive polarization (+0.4 V) enhances bacterial capture through electrostatic attraction, whereas negative polarization (−0.4 V) repels bacteria from the surface (***Figure 39a***). During negative polarization, a clear decrease in the SPR signal was observed, indicating bacterial desorption (**Figure 39b**). In contrast, applying a +0.4 V polarization produced a significant increase in signal intensity, confirming the specific accumulation of *E. coli* at the electrode interface (Figure 39b). This behavior is consistent with previous findings showing that SPR signal intensity is modulated by the proximity and density of biological analytes at the gold surface. [20].

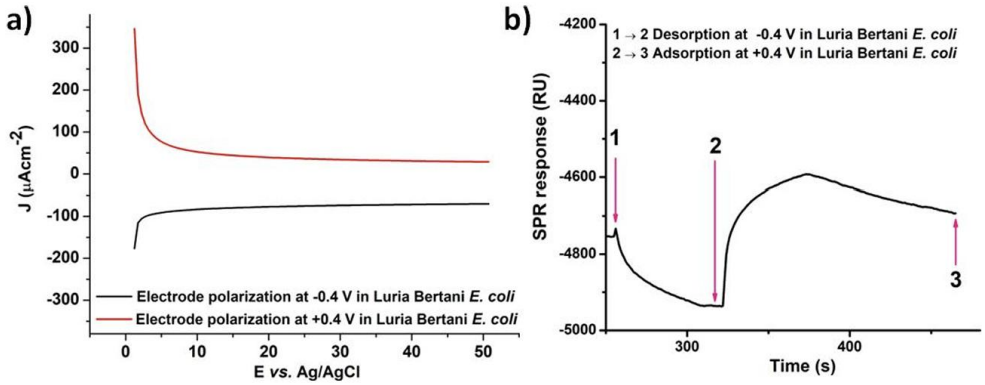


Figure 39. *(a) Current density–potential curves during electrode polarization at −0.4 V and +0.4 V in E. coli Luria–Bertani medium; (b) SPR response as a function of time, illustrating bacterial desorption at −0.4 V and adsorption at +0.4 V.*

6.3.3. Sensitivity and Linearity of the EC-SPR Response in *E. coli* Detection on the Modified Gold Electrode

The surface sensitivity was calculated from the slope of the calibration curve. The obtained value was 0.0043 R.U./(CFU·mL^{-1}). The very high correlation coefficient ($R^2 = 0.996$) indicates excellent linearity over the investigated concentration range. To evaluate the analytical performance of the EC-SPR detection platform, the limit of detection (LoD) and the limit of quantification (LoQ) were calculated based on the calibration data, using the formulas reported in the literature [21]. A linear regression model was constructed for the SPR response as a function of *E. coli* concentration, yielding a slope of 0.0043 R.U./(CFU·mL^{-1}) and a residual standard deviation (σ) of 3.70 R.U.

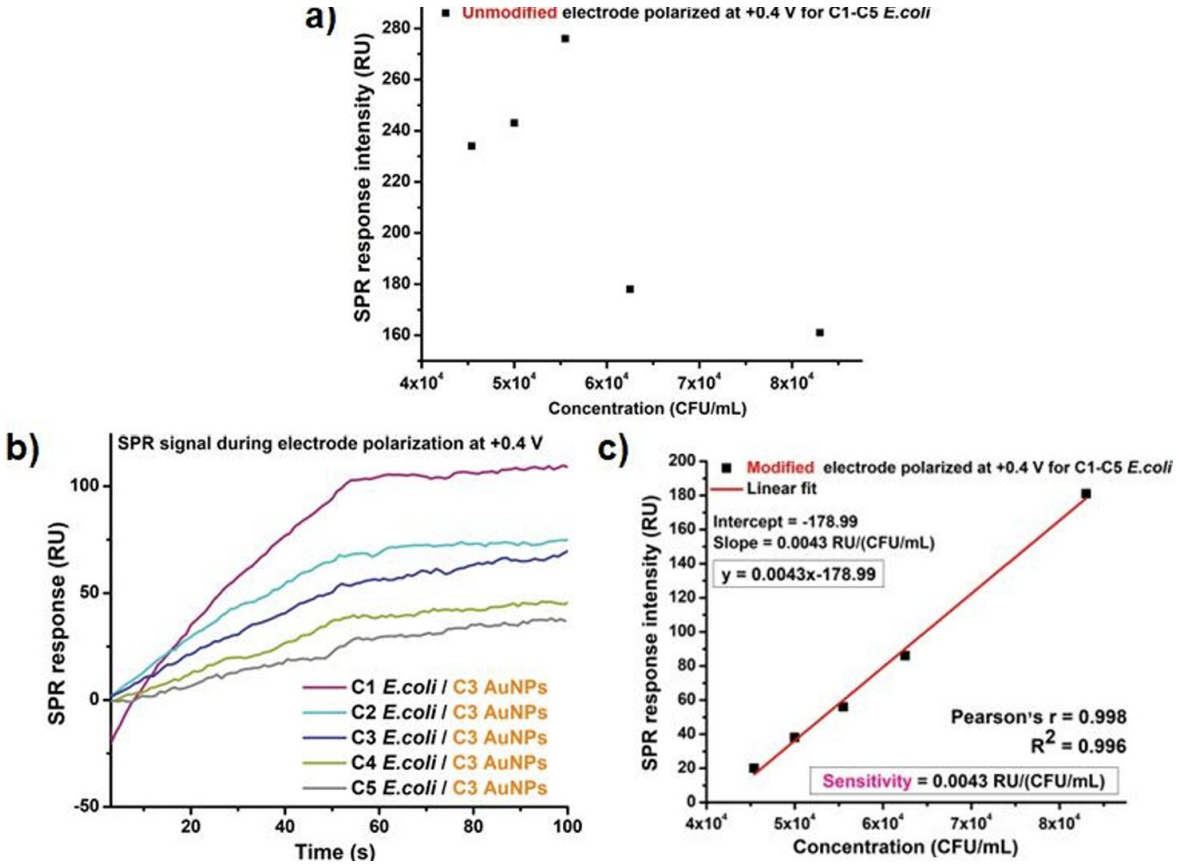


Figure 43. *(a) SPR response intensity for each bacterial concentration without nanoparticles; (b) SPR signal for each bacterial concentration in the presence of the C3 AuNPs sample; (c) calibration curve corresponding to the SPR signal in (b).*

Based on these calculations, a LoD value of 0.454 × 10^5 CFU·mL^{-1} and a LoQ value of 0.830 × 10^5 CFU·mL^{-1} were obtained. These values provide clear evidence of the suitability of the system for detecting low concentrations and small volumes of *E. coli* in aqueous samples. Such a linear response is essential for real-world applications, where accurate quantification of bacterial contamination is critical. The achieved sensitivity and correlation are comparable to

or superior to those reported for other EC-SPR systems for *E. coli* detection. Notably, these performances were achieved without the use of biological recognition elements such as antibodies or aptamers, which simplifies the testing procedure and improves the lifetime and robustness of the developed detection platform.

Chapter 7 develops an amoxicillin detection platform based on ZnO derived from *Bombyx mori* silk fibroin and $Zn(NO_3)_2$, yielding fibrous, nanoscale structures with wurtzite crystalline phases, as confirmed by SEM, FT-IR, and XRD. These nanostructures were incorporated into a Nafion film deposited on a glassy carbon electrode, and various parameters (ZnO concentration, drying time) were optimized. CV and DPV were compared for amoxicillin detection, with DPV proving superior. A calibration curve was constructed, and a LoD value of 0.02 µM was obtained, comparable to or better than values reported in the literature, demonstrating the sensor's potential for antibiotic monitoring.

7.3.4. Calibration Curve

To obtain the calibration curve, AMX solutions in PBS with concentrations ranging from 5 to 110 µM were prepared. An increase in peak height corresponding to increasing amoxicillin concentration is observed in ***Figure 52b***. The oxidation reaction of AMX (Figure 52a) at the GC/Nafion/ZnO 9 electrode results in a calibration curve with excellent linearity ($R^2 = 0.998$), as shown in the inset of ***Figure 52b***.

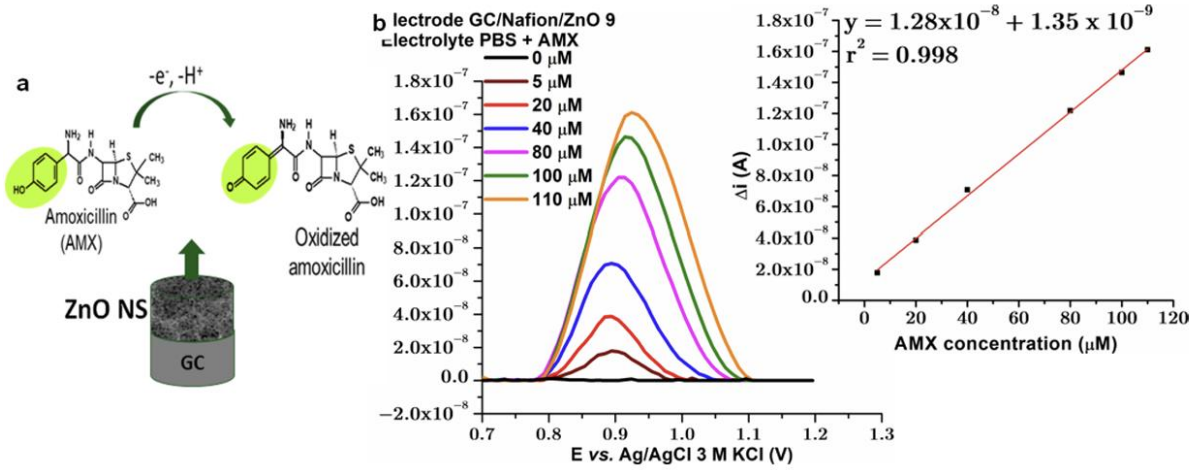


Figure 52. *(a) Redox reaction of amoxicillin; (b) DPV curves in PBS solution containing amoxicillin at six different concentrations and the corresponding calibration curve obtained using the GC/Nafion/ZnO 9 electrode.*

The LoD and LoQ, corresponding to the limit of detection and the limit of quantification, were calculated using the linear regression method. The LoD was 0.02 µM, while the LoQ was 0.05 µM.

Chapter 8 focuses on the development of a non-enzymatic detection platform for D-fructose, using glassy carbon electrodes (GCE) modified with polypyrrole (PPy), Nafion, and Carbon Quantum Dots (CQDs) electrochemically synthesized from graphite or carbon rods. The composition, electrochemical conditions, and different electrode architectures are described. The results demonstrate that the simple introduction of CQDs does not guarantee an increase in sensitivity. Optimal performance is achieved only when morphology, composition, and ionic/electronic transport are simultaneously tuned, and for the optimized architecture a linear response is obtained within biomedically relevant concentration ranges of D-fructose.

8.1.5. Characterization of Carbon Quantum Dots

A remarkable difference in fluorescence was observed between the two CQD synthesis methods. This difference became evident after exposure to a UV lamp with a wavelength of 365 nm. Nanoparticles synthesized in a KOH and ethanol solution exhibited fluorescence mainly at the surface of the solution, compared to the rest of the solution where the quantum dots were aggregated (***Figure 58a***). In contrast, particles synthesized in an aqueous solution of citric acid and NaOH showed the best fluorescence throughout the entire solution, displaying a light blue color (***Figure 58b***). According to the literature [22, 23], the size of CQDs synthesized by the first method ranges between 3–5 nm, as inferred from their green–orange emission color. For CQDs synthesized by the second method, the particle size is in the range of 2–2.5 nm.

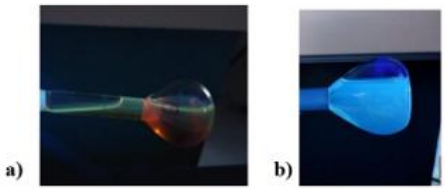


Figure 58. *CQDs synthesized in: (a) KOH and ethanol solution, and (b) citric acid and NaOH solution.*

8.2. Results and Discussion

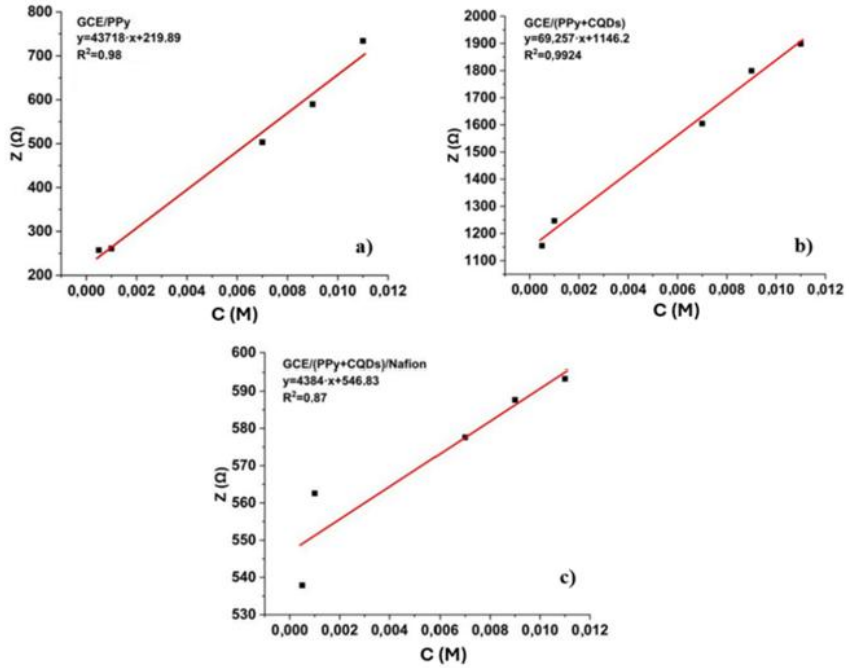


Figure 63. *Calibration curves corresponding to the samples: (a) GCE/PPy, (b) GCE/PPy/(PPy + 3 mL CQDs), (c) GCE/PPy/(PPy + 3 mL CQDs)/Nafion.*

Pentru electrodul de carbon vitros modificat cu polipirol și CQDs, GC/(PPy + CQDs), inserarea CQD-urilor în soluția de Py în timpul polimerizării și modificării suprafeței electrodului a îmbunătățit liniaritatea răspunsul electrodului probabil datorita unei adsorbții slabă–moderată și reversibilă a D-fructozei la suprafață care a condus la o mai buna fixare pe suprafață și la îmbunătățirea semnalului electrodului. Pentru curba de calibrare obținută coeficientul de determinare R^2 este 0,9924.

Chapter 9 describes the main conclusions drawn from the doctoral research.

The thesis integrates, within a unified framework, the processes of modification, characterization, and application of functionalized surfaces for the control, modulation, and detection of biologically active agents. The approach addressed both the optimization of the material–biological system interface and the development of analytical platforms capable of providing rapid and sensitive responses in relevant biomedical contexts.

Conclusions on the Control and Modulation of Antibacterial Activity against *E. coli* on Titanium Alloy Surfaces

The control of antibacterial activity against *E. coli* was achieved by modulating the surface properties of a titanium alloy (Ti50Zr). It was demonstrated that the antibacterial response of a metallic implant is not governed by a single factor, but rather by a set of surface

properties such as wettability and surface energy, surface charge, nanoscale roughness, and morphology, which together regulate bacterial attachment, membrane stress, and eventual cell death.

This study provides a comprehensive analysis of the antibacterial performance against *E. coli* of Ti50Zr alloys modified by anodic oxidation to form oxide layers—compact oxide (CO), nanotubes (NT), and nanochannels (NC)—and by pulsed electrodeposition (ZnO coatings), highlighting the multifactorial interactions governing bacterial adhesion and inhibition. The Ti50Zr NC structure exhibited the highest antibacterial efficiency, with an inhibition rate of 60%, attributed to its nanostructured morphology. ZnO coating further amplified antibacterial activity, with Ti50Zr NCZnO showing the highest inhibition rate (75%), suggesting a synergistic effect between surface nanostructuring and ZnO-mediated bacterial inactivation.

The antibacterial mechanism is primarily determined by a combination of surface interactions (arising from surface nanostructuring), ZnO-mediated oxidative stress, and electrostatic interactions, rather than by a single dominant factor. These results emphasize the importance of surface engineering through nanostructuring and ZnO integration for controlling antibacterial properties. The findings highlight the complex interplay between surface morphology, physicochemical properties, and ZnO-mediated bacterial interactions, offering valuable insights for the development of next-generation antibacterial biomaterials for medical applications.

Conclusions on the EC-SPR Platform for *E. coli* Detection

This study involved the modification of a gold electrode with gold nanoparticles (AuNPs) produced through an eco-friendly phytochemical process using broccoli leaf extract (*Brassica oleracea*) to construct an electrochemically coupled surface plasmon resonance (EC-SPR) detection platform for *E. coli*. The integration of phytosynthesized AuNPs into the active layer of the EC-SPR sensor significantly increased the opto-electrochemical sensitivity toward *E. coli*, demonstrating a linear and reproducible response without the need for antibodies or aptamers.

The EC-SPR system enabled rapid, label-free bacterial detection with low LoD and LoQ values, allowing real-time monitoring of biological contamination. This method provides a sustainable and environmentally friendly alternative to classical immunological procedures, reinforcing the concept of biofunctional sensors integrated into biomedical materials.

Conclusions on the Electrochemical Platform for Amoxicillin Detection

A novel electrochemical detection system based on ZnO nanostructures grown within a natural silk fibroin matrix was developed by modifying a glassy carbon electrode with these

nanostructures. The ZnO nanostructures obtained from silk fibroin exhibited optical and crystalline properties characteristic of the wurtzite phase, favorable for charge transfer.

The highly porous, fibrillar ZnO nanostructures were deposited onto the glassy carbon electrode surface by incorporation into a Nafion polymer matrix. Their integration into a Nafion film improved the selectivity and stability of the detection system. Differential pulse voltammetry was optimized for amoxicillin detection, achieving a detection limit of 0.02 μM, comparable to or better than values reported in the literature. The proposed platform shows strong potential for antibiotic monitoring in biological fluids and environmental samples and is compatible with integration into portable systems.

Conclusions on D-Fructose Detection Using CQD-Modified Electrodes

This study focused on the development of a non-enzymatic detection system for D-fructose using carbon-based electrodes modified with polypyrrole and Nafion, with the addition of carbon quantum dots (CQDs). Unmodified glassy carbon electrodes and modified electrodes were tested by electrochemical impedance spectroscopy at different D-fructose concentrations. The unmodified glassy carbon electrode did not show a correlation between impedance response and D-fructose concentration, preventing the construction of a specific calibration curve.

In contrast, the polypyrrole-modified electrode (GCE/PPy) exhibited a calibration curve with a determination coefficient R^2 of 0.986, due to a significantly improved response compared to the unmodified electrode. Oxidized polypyrrole (PPy^+) possesses a positively charged backbone that enables stronger interactions with D-fructose through hydrogen bonding.

For the polypyrrole and CQD-modified electrode (GCE/(PPy + CQDs)), the incorporation of CQDs into the pyrrole solution during polymerization and electrode surface modification improved response linearity, likely due to weak-to-moderate and reversible adsorption of D-fructose at the surface, leading to better surface fixation and enhanced signal. This improvement was reflected by a determination coefficient R^2 of 0.9924 obtained from the calibration curve. The addition of Nafion to the film structure did not result in further signal enhancement. Further investigations are required to optimize D-fructose detection by adjusting operating parameters and the molar ratios of the solutions used for electrode surface modification.

References

[1] O. Galasso, A. Crinisio, A. Bartoli, B. Moretti, Advances and Challenges in Orthopedic Implant-Associated Infections, Healthcare, MDPI, 2024, p. 1819.

[2] A. Mishra, A. Aggarwal, F. Khan, Medical device-associated infections caused by biofilm-forming microbial pathogens and controlling strategies, Antibiotics 13(7) (2024) 623.

[3] O. Grari, S. Ezrari, I. El Yandouzi, E. Benaissa, Y.B. Lahlou, M. Lahmer, A. Saddari, M. Elouennass, A. Maleb, A comprehensive review on biofilm-associated infections: Mechanisms, diagnostic challenges, and innovative therapeutic strategies, The Microbe 8 (2025) 100436.

[4] Z. Hu, X. Yin, G. Fan, X. Liao, Global Trends in Orthopedic Biofilm Research: A Bibliometric Analysis of 1994-2022, Journal of Multidisciplinary Healthcare (2024) 3057-3069.

[5] S. Sharma, J. Mohler, S.D. Mahajan, S.A. Schwartz, L. Bruggemann, R. Aalinkeel, Microbial biofilm: a review on formation, infection, antibiotic resistance, control measures, and innovative treatment, Microorganisms 11(6) (2023) 1614.

[6] A. Zhao, J. Sun, Y. Liu, Understanding bacterial biofilms: From definition to treatment strategies, Frontiers in cellular and infection microbiology 13 (2023) 1137947.

[7] F. Sivori, I. Cavallo, M. Truglio, L. Pelagalli, V. Mariani, G. Fabrizio, E. Abril, I. Santino, P.A. Fradiani, M. Solmone, Biofilm-mediated antibiotic tolerance in Staphylococcus aureus from spinal cord stimulation device-related infections, Microbiology Spectrum 12(12) (2024) e01683-24.

[8] L. Kadirvelu, S.S. Sivaramalingam, D. Jothivel, D.D. Chithiraiselvan, D.K. Govindarajan, K. Kandaswamy, A review on antimicrobial strategies in mitigating biofilm-associated infections on medical implants, Current Research in Microbial Sciences 6 (2024) 100231.

[9] M.A. Azad, R. Patel, Practical Guidance for Clinical Microbiology Laboratories: Microbiologic diagnosis of implant-associated infections, Clinical Microbiology Reviews 37(2) (2024) e00104-23.

[10] S. Liang, M. Hu, B. Li, D. Xia, C. Liang, F. Peng, D. Wang, Smart implant with bacteria monitoring and killing ability for orthopedic applications, ACS Applied Materials & Interfaces 15(25) (2023) 29889-29901.

[11] A.C. Scalia, Z. Najmi, Targeting Bacterial Biofilms on Medical Implants: Current and Emerging Approaches, Antibiotics 14(8) (2025) 802.

[12] M. Alam, A.M. Asiri, M.M. Rahman, M. Islam, Fabrication of sensitive D-fructose sensor based on facile ternary mixed ZnO/CdO/SnO2 nanocomposites by electrochemical approach, Surfaces and Interfaces 19 (2020) 100540.

[13] S. Madhu, S. Ramasamy, J. Choi, Recent developments in electrochemical sensors for the detection of antibiotic-resistant bacteria, Pharmaceuticals 15(12) (2022) 1488.

[14] D.J. Davidson, D. Spratt, A.D. Liddle, Implant materials and prosthetic joint infection: the battle with the biofilm, EFORT open reviews 4(11) (2019) 633-639.

[15] E.C. Rodríguez-Merchán, D.J. Davidson, A.D. Liddle, Recent strategies to combat infections from biofilm-forming bacteria on orthopaedic implants, International journal of molecular sciences 22(19) (2021) 10243.

[16] A. Constantinescu, C. Ungureanu, C. Dumitriu, C. Pirvu, Complex interplay of surface properties in modulating antibacterial activity of Ti50Zr alloys, RSC advances 15(20) (2025) 15738-15747.

[17] J. Jenkins, J. Mantell, C. Neal, A. Gholinia, P. Verkade, A.H. Nobbs, B. Su, Antibacterial effects of nanopillar surfaces are mediated by cell impedance, penetration and induction of oxidative stress, Nature communications 11(1) (2020) 1626.

[18] A. Pirouz, I. Papakonstantinou, M. Michalska, Antimicrobial mechanisms of nanopatterned surfaces—a developing story, Frontiers in Chemistry 12 (2024) 1354755.

[19] B. Zudyte, Z. Luksiene, Visible light-activated ZnO nanoparticles for microbial control of wheat crop, Journal of Photochemistry and Photobiology B: Biology 219 (2021) 112206.

[20] J. Homola, Surface plasmon resonance sensors for detection of chemical and biological species, Chemical reviews 108(2) (2008) 462-493.

[21] S.A. Leau, C. Lete, C. Matei, S. Lupu, Electrochemical sensing platform based on metal nanoparticles for epinephrine and serotonin, Biosensors 13(8) (2023) 781.

[22] S. Sultana, M.S. Alam, Confinement effects and tunability of quantum dots within strong confinement regime, 2015 IEEE International WIE Conference on Electrical and Computer Engineering (WIECON-ECE), IEEE, 2015, pp. 31-34.

[23] A. Abbas, Fluorescent Nanomaterials from Biomass: Synthesis and Applications, Newcastle University, 2021.

Functionalized platforms for the control, modulation, and detection of biologically active agents

Acknowledgements

First and foremost, I would like to express my sincere gratitude to Professor Cristian Pîrvu, who represents a role model that I will always strive to follow. I thank him for being by my side regardless of the circumstances and for his unconditional support in everything I set out to achieve. I am also grateful for his constant guidance throughout the completion of this thesis and for his continuous encouragement and optimism.

My thanks also go to my colleagues from the Department of General Chemistry, alongside whom I had the privilege to work. I would like to address special thanks to Associate Professor Camelia Ungureanu for her support. I thank Professor Nicoleta Badea for her kindness and openness on every occasion, as well as Associate Professors Grațiela Tihan and Roxana Zgârian for their generosity and help whenever I needed it.

I would also like to thank Professor Cătălin Zaharia and Associate Professor Bianca Gălățeanu for their availability and promptness whenever I presented my doctoral thesis reports.

I would also like to thank my friends, who stood by me with encouragement, patience, and unconditional moral support. In particular, I would like to thank my friends Cristina Secu, Mihai Dumitru, Sorina Alexandra Leau, and Ana-Maria Pușcașu.

Last but not least, I am deeply grateful to my family for the support they have always provided. Their encouragement has been the foundation upon which my entire professional and personal development has been built.

Alexandra Constantinescu